

Electric-circuit simulation of the Schrödinger equation and non-Hermitian quantum walks

Motohiko Ezawa

Department of Applied Physics, University of Tokyo, Hongo 7-3-1, 113-8656, Japan

Recent progress has witnessed that various topological physics can be simulated by electric circuits under alternating current. However, it is still a nontrivial problem if we may simulate the dynamics subject to the Schrödinger equation based on electric circuits. In this work, we reformulate the Kirchhoff law in one dimension in the form of the Schrödinger equation. As a typical example, we investigate quantum walks in LC electric circuits. We also investigate how quantum walks are different in topological and trivial phases by simulating the Su-Schrieffer-Heeger model in electric circuits. We then generalize them to include dissipation and nonreciprocity by introducing resistors, which produce non-Hermitian effects. We point out that the time evolution of one-dimensional quantum walks is exactly solvable with the use of the generating function made of the Bessel functions. Our results raise a possibility constructing quantum computers based on electric circuits.

Electric circuits have demonstrated their usefulness in the field of condensed-matter physics since they can simulate various topological physics^{1–16}. It has been proved that the circuit Laplacian and the tight-binding Hamiltonian have a one-to-one correspondence when an alternating current is applied^{1,2}. It is yet an open problem whether the dynamics governed by the Schrödinger equation can be simulated by electric circuits. A simplest dynamical problem would be a one-dimensional quantum walk, which we wish to explore.

Quantum walk is a diffusion process governed by the Schrödinger equation^{17–22}. As a function of time, it spreads linearly and faster than a classical random walk which spreads proportional to the square root of time^{23,24}. Quantum walk is a basic concept in quantum information processes including quantum search²⁵, universal quantum computation^{26,27} and quantum measurement²⁸. It is realized in photonic lattice^{29–32}, wave guide³³ and nuclear-magnetic-resonance^{34,35}.

In this paper, we first reformulate the telegrapher equation in the form of the Schrödinger equation, implying that the Schrödinger equation is simulated by electric circuits. Second, we solve the Schrödinger equation analytically to describe a quantum walker. Third, we investigate how quantum walks are different in topological and trivial phases. For this purpose we propose an electric-circuit simulation of the Su-Schrieffer-Heeger (SSH) model. Topological and trivial phases are well distinguished by the time evolution of a quantum walk starting from the edge. Finally, we study a non-reciprocal non-Hermitian quantum walk, where we find that a quantum walker linearly displaces while the variance increases only linearly as a function of time. It is highly contrasted to a reciprocal quantum walk. Our results will be a basis for future quantum computations based on electric circuits.

Quantum walk based on LC electric circuits: Our system is a chain of electric circuit shown in Fig.1. It describes the telegrapher equation provided the system is homogeneous. An inhomogeneous circuit is constructed by choosing the sample parameters different depending on the position in a chain. An electric circuit is characterized by the Kirchhoff current and

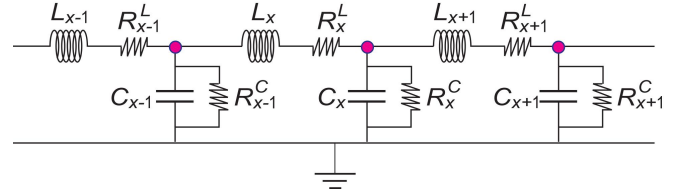


FIG. 1: Illustration of an electric circuit realizing an inhomogeneous telegrapher equation.

voltage laws,

$$C_x \frac{d}{dt} V_x = I_{x-1} - I_x - R_x^C V_x, \quad (1)$$

$$L_x \frac{d}{dt} I_x = V_x - V_{x+1} - R_x^L I_x. \quad (2)$$

They are combined into a second-order differential equation by deleting I or V in the standard treatment³⁶.

We first analyze the homogeneous case such that $C_x = C$, $L_x = L$, $R_x^L = R^L$ and $R_x^C = R^C$. Here, we reformulate the set of equations (1) and (2) in the form of the Schrödinger equation $i\partial_t \Psi_k = H(k) \Psi_k$, where $\Psi_k = (V_k, I_k)^t$ and

$$H(k) = \begin{pmatrix} -iR^C & -\frac{i}{C}(1 - e^{-ik}) \\ \frac{i}{L}(1 - e^{ik}) & -iR^L \end{pmatrix}. \quad (3)$$

This Hamiltonian is non-Hermitian. By making a scale transformation

$$V_k = \alpha \mathcal{V}_k, \quad I_k = \beta \mathcal{I}_k \quad (4)$$

with $\alpha/\beta = \sqrt{L/C}$, we can transform it into the maximally Hermitianized form $i\partial_t \psi_k = \mathcal{H}(k) \psi_k$, where $\psi_k = (\mathcal{V}_k, \mathcal{I}_k)^t$ and

$$\mathcal{H}(k) = \begin{pmatrix} -iR^C & -\frac{i}{\sqrt{LC}}(1 - e^{-ik}) \\ \frac{i}{\sqrt{LC}}(1 - e^{ik}) & -iR^L \end{pmatrix}. \quad (5)$$

Indeed, this Hamiltonian is Hermitian if all resistors are removed ($R^C = R^L = 0$). The energy spectrum is given by

$$E = -i \frac{R^C + R^L}{2} \pm \sqrt{\frac{4}{LC} \sin^2 k - \left(\frac{R^C - R^L}{2} \right)^2}. \quad (6)$$

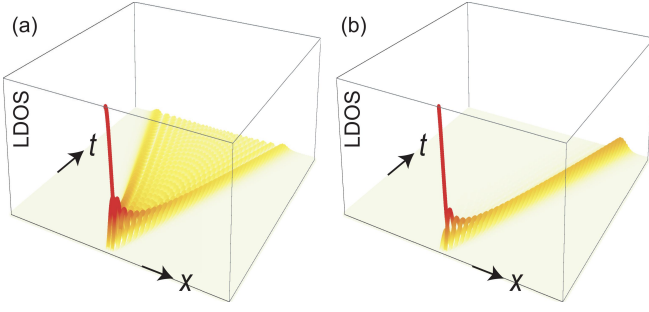


FIG. 2: (a) Time evolution of a quantum walk. (b) Time evolution of a quantum walk with nonreciprocity ($\gamma = 1.25$) and dissipation ($R = 0.4$). The vertical axis is the LDOS. We have set $L_x = C_x = 1$.

The dynamics is solved as $\psi_k(t) = e^{i\mathcal{H}(k)t}\psi_k(0)$.

The Schrödinger equation $i\partial_t\psi_k = \mathcal{H}(k)\psi_k$ is transformed into the real space as

$$i\frac{d}{dt}\psi_x = \frac{i}{\sqrt{LC}}\psi_{x-1} - iR\psi_x - \frac{i}{\sqrt{LC}}\psi_{x+1}, \quad (7)$$

where we have defined

$$\psi_x = (\cdots, \mathcal{V}_{x-1}, \mathcal{I}_{x-1}, \mathcal{V}_x, \mathcal{I}_x, \mathcal{V}_{x+1}, \mathcal{I}_{x+1}, \cdots)^t. \quad (8)$$

We start with a quantum walker starting from $x = 0$ at $t = 0$. Namely, we solve the Schrödinger equation by imposing the initial condition $\psi_x = \delta_{x0}$ at $t = 0$. For simplicity we set $R^L = R^C = R$. The analytic solution is obtained as

$$\psi_x = e^{-Rt} J_{|x|} \left(\frac{2}{\sqrt{LC}} t \right), \quad (9)$$

where J_x is the Bessel function. We show the time evolution of the eigenstate in Fig.2(a). It linearly spreads as a function of time, which is a characteristic feature of quantum walk^{23,24}. The eigenstate is observable by measuring the voltage and the current.

We discuss analytically how the wave packet describing the quantum walker spreads throughout the lattice as shown in Fig.2(a). We define a generating function by²⁴

$$G(k) = \sum_{x=-\infty}^{\infty} |\psi_x(t)|^2 e^{kx}. \quad (10)$$

By using the sum formula of the Bessel function,

$$\sum_{x=-\infty}^{\infty} J_{|x|}^2(t) e^{kx} = I_0 \left(t\sqrt{2(\cosh k - 1)} \right), \quad (11)$$

we find

$$G(k) = e^{-2Rt} I_0 \left(2t\sqrt{\frac{2(\cosh k - 1)}{LC}} \right), \quad (12)$$

where I_0 is the modified Bessel function. The n -th moment is calculated as

$$\langle x^n \rangle = \lim_{k \rightarrow 0} \frac{d^n G(k)}{dk^n}. \quad (13)$$

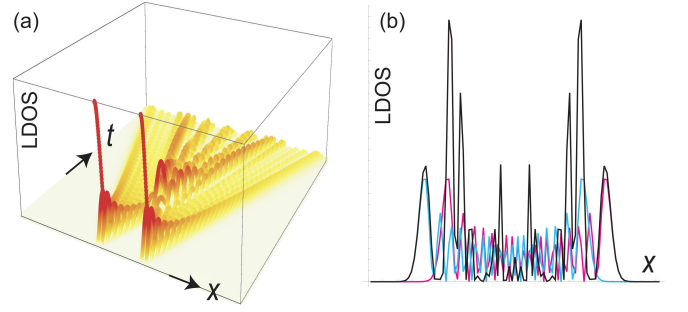


FIG. 3: Electric circuit simulation of interference experiment. (a) Time evolution of two quantum walkers starting from two points. (b) Absolute value of the LDOS at a fixed time t . The magenta (cyan) curve represents the probability to find the right (left) walker at a certain point, while the black curve represents the probability to find a walker at a certain point. The black curve clearly forms an interference pattern. We have set $L = C = 1$, $R = 0$ and $t = 30$.

The total density decreases as

$$\langle 1 \rangle = G(0) = e^{-2Rt} \quad (14)$$

in the presence of the dissipation R . Indeed, we obtain $\sum_{x=-\infty}^{\infty} |\psi_x(t)|^2 = 1$ for $R = 0$. The mean position is $\langle x \rangle = 0$, while the variance is

$$\langle x^2 \rangle = \frac{4t^2}{LC} e^{-2Rt}. \quad (15)$$

Hence, in the absence of the dissipation ($R = 0$), the eigenfunction diffuses linearly as a function of time, which is a manifestation of a quantum walk^{23,24}.

Interference experiment: We analyze the problem of two quantum walkers. Let their starting points be $x \pm x_0$ at $t = 0$. The eigen function is simply given by a linear superposition of two eigenstates of the type (9),

$$\psi_x = \psi_x^+ + \psi_x^-, \quad (16)$$

where

$$\psi_x^\pm = e^{-Rt} J_{|x \pm x_0|} \left(\frac{2}{\sqrt{LC}} t \right). \quad (17)$$

We show the absolute value of ψ_x for a fixed time in Fig.3(b). An interference pattern is clearly observed.

Quantum walk in inhomogeneous system: We generalize the results to an inhomogeneous system. By making a spatial dependent scale transformation $\mathcal{V}_x = \alpha_x \mathcal{V}_x$ and $\mathcal{I}_x = \beta_x \mathcal{I}_x$ in (1) and (2) we obtain equations

$$i\frac{d}{dt}\mathcal{V}_x = \frac{i\beta_{x-1}}{\alpha_x C_x} \mathcal{I}_{x-1} - iR_x^C \mathcal{V}_x - \frac{i\beta_x}{\alpha_x C_x} \mathcal{I}_x, \quad (18)$$

$$i\frac{d}{dt}\mathcal{I}_x = \frac{i\alpha_x}{\beta_x L_x} \mathcal{V}_x - iR_x^L \mathcal{I}_x - \frac{i\alpha_{x+1}}{\beta_x L_x} \mathcal{V}_{x+1}. \quad (19)$$

These equations lead to a non-Hermitian Hamiltonian as they stand.

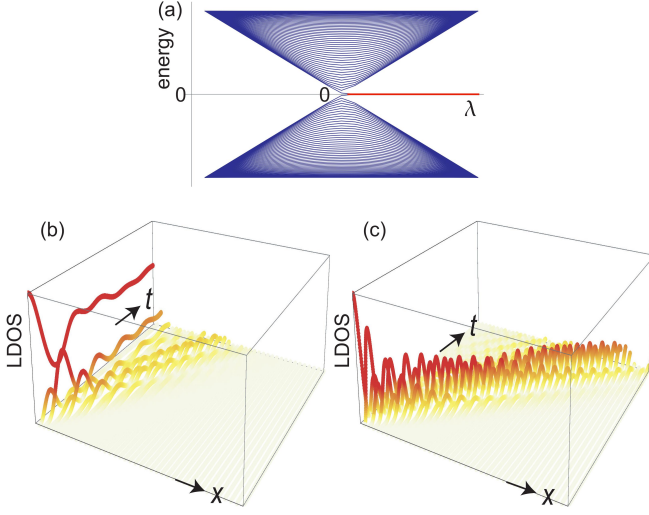


FIG. 4: (a) Energy spectrum as a function of λ . There are "zero-energy" edge states indicated by a red line in the topological phase ($\lambda > 0$), while there are no edge states in the trivial phase ($\lambda < 0$). (b) Time evolution of a quantum walk in the topological phase ($\lambda = 0.5$), and (c) that in the trivial phase ($\lambda = -0.5$). A quantum walk does not diffuse for the topological phase, while it diffuses for the trivial phase.

It is intriguing that we are able to construct a maximally Hermitianized Hamiltonian from these equations. By setting $\alpha_x = \sqrt{L_1 C_1 / C_x}$ and $\beta_x = \sqrt{L_1 C_1 / L_x}$, the set of equations acquires a maximally Hermitianized form,

$$i \frac{d}{dt} \mathcal{V}_x = \frac{i}{\sqrt{L_{x-1} C_x}} \mathcal{I}_{x-1} - i R_x^C \mathcal{V}_x - \frac{i}{\sqrt{L_x C_x}} \mathcal{I}_x, \quad (20)$$

$$i \frac{d}{dt} \mathcal{I}_x = \frac{i}{\sqrt{L_x C_x}} \mathcal{V}_x - i R_x^L \mathcal{I}_x - \frac{i}{\sqrt{L_x C_{x+1}}} \mathcal{V}_{x+1}. \quad (21)$$

When we set $R_x^C = R_x^L = R$ for simplicity, the corresponding tight-binding Hamiltonian has a particularly simple form,

$$H = \sum_x t_x (|\psi_x\rangle \langle \psi_{x+1}| + |\psi_{x+1}\rangle \langle \psi_x|) - iR |\psi_x\rangle \langle \psi_x|, \quad (22)$$

with $t_{2x-1} = 1/\sqrt{L_x C_x}$ and $t_{2x} = 1/\sqrt{L_{x/2} C_{x/2+1}}$. Here, t_x represents the hopping parameter between two sites x and $x+1$. The inverse solutions are given by

$$\frac{L_x}{L_1} = \frac{\prod_{j=1}^{x-1} t_{2j}}{\prod_{j=1}^{x-1} t_{2j+1}}, \quad \frac{C_x}{C_1} = \frac{\prod_{j=1}^{x-1} t_{2j-1}}{\prod_{j=1}^{x-1} t_{2j}}. \quad (23)$$

Consequently, it is possible to arrange capacitors C_x and inductors L_x to reproduce various tight-binding models with arbitrary hopping parameters t_x .

Quantum walks in topological and trivial phases: We proceed to investigate how quantum walks are different in topological and trivial phases. The simplest model possessing

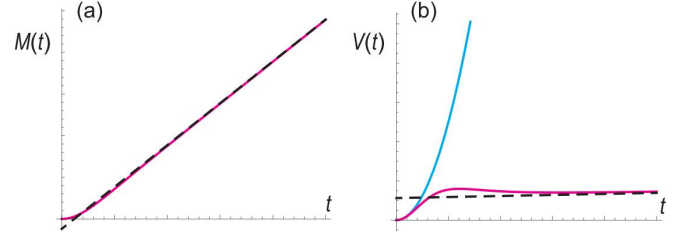


FIG. 5: (a) Time evolution of the mean value $M(t)$. (b) Time evolution of the variance $V(t)$. Cyan curves represent a reciprocal quantum walk, while magenta curves represent a nonreciprocal with $\gamma = 1.1$ quantum walk. Black dotted lines are asymptotic formula for $t \rightarrow \infty$.

these phases is given by the SSH model. The SSH model is given by the Hamiltonian (22) together with $R = 0$ and

$$t_x = t + (-1)^x \lambda. \quad (24)$$

The electric circuit is constructed by choosing inductors and capacitors satisfying (23). The energy spectrum is shown as a function of λ in Fig.4(a). There are "zero-energy" edge states for $\lambda > 0$, signaling that the system is topological, while the system is trivial for $\lambda < 0$ with no edge states. The edges are said topological for $\lambda > 0$. These two phases are clearly distinguished by examining quantum walks. Let a quantum walker start from one of the edges. Namely, we consider the initial state chosen to be perfectly localized at one edge. In the topological phase, a nonzero local density of state (LDOS) remains at the edge as shown in Fig.4(b), while the LDOS rapidly decreases for the trivial phase as shown in Fig.4(c).

These behaviors are understood analytically as follows. By expanding the initial state in terms of the eigenstates as

$$\psi_x^{\text{ini}} = \sum_j c_j \psi_x^{(j)}, \quad (25)$$

the dynamics is given by

$$\psi_x(t) = \sum_j c_j e^{iE_j t} \psi_x^{(j)}, \quad (26)$$

where E_j is the j -th energy, and $\psi_x^{(j)}$ is the eigenstate with the energy E_j . For the topological phase the coefficient c_j has the largest value for the edge state, which has no dynamics. It results in a nonzero LDOS at the edge as in Fig.4(b). On the other hand, there is no dominant c_j for the trivial states, which results in the rapid spread of the initial state in Fig.4(c).

Non-Hermitian nonreciprocal quantum walk: Next, by setting

$$\alpha_x = \gamma^{2x} \sqrt{\frac{L_1 C_1}{C_x}}, \quad \beta_x = \gamma^{2x+2} \sqrt{\frac{L_1 C_1}{L_x}} \quad (27)$$

in (4), we construct a non-Hermitian nonreciprocal model^{10,37-39},

$$H = \sum_x t_x \left(\gamma |\psi_x\rangle \langle \psi_{x+1}| + \frac{1}{\gamma} |\psi_{x+1}\rangle \langle \psi_x| \right) - iR |\psi_x\rangle \langle \psi_x|, \quad (28)$$

where the parameter γ represents the nonreciprocity. The Schrödinger equation is given by

$$i\frac{d}{dt}\psi_x = \frac{i\gamma}{\sqrt{LC}}\psi_{x-1} - iR\psi_x - \frac{i}{\gamma\sqrt{LC}}\psi_{x+1}. \quad (29)$$

We find an analytic solution

$$\Psi_x(t) = \gamma^x e^{-Rt} J_{|x|}\left(\frac{2}{\sqrt{LC}}t\right). \quad (30)$$

The generating function is

$$G(k) = e^{-2Rt} I_0\left(2t\sqrt{\frac{\gamma^2 e^k + e^{-k}/\gamma^2 - 2}{LC}}\right). \quad (31)$$

We find the total LDOS as

$$\sum_{x=-\infty}^{\infty} |\psi_x(t)|^2 = e^{-2Rt} I_0\left(2t\sqrt{\frac{\gamma^2 + 1/\gamma^2 - 2}{LC}}\right). \quad (32)$$

Indeed, it reproduces the result $\langle 1 \rangle \equiv \sum_{x=-\infty}^{\infty} |\psi_n(t)|^2 = 1$ for the case $\gamma = 1$ and $R = 0$. The mean value is defined by $M(\Psi) = \langle x \rangle / \langle 1 \rangle$, where we note $\langle 1 \rangle \neq 1$ in general, whose asymptotic behaviors is given by

$$\lim_{t \rightarrow \infty} M(\Psi) = \frac{\gamma^2 - 1/\gamma^2}{4\left(\gamma^2 + \frac{1}{\gamma^2} - 2\right)} \left(\frac{4t}{\sqrt{LC}} \sqrt{\gamma^2 + \frac{1}{\gamma^2} - 2} - 1\right). \quad (33)$$

The variance is given by $V(\Psi) = \langle x^2 \rangle / \langle 1 \rangle - M^2(\Psi)$, which reads

$$\lim_{t \rightarrow \infty} V(\Psi) = \frac{1}{2} \left(\frac{\gamma^2}{(1 - \gamma^2)^2} + \sqrt{\gamma^2 + \frac{1}{\gamma^2} - 2} \frac{t}{\sqrt{LC}} \right), \quad (34)$$

where we have used the asymptotic formula of the modified Bessel function $\lim_{t \rightarrow \infty} I_0(t) = e^t / \sqrt{2\pi t}$. We show the time evolution of the mean and variance in Fig.5. The asymptotic behaviors well reproduce the analytic results.

We have shown that the one-dimensional Schrödinger equation is simulated by electric circuits. As a typical example, we have studied quantum walks. Dissipative and nonreciprocal quantum walks are realized by tuning the sample parameters. In a nonreciprocal quantum walk, the variance is proportional to time which is smaller than a reciprocal quantum walk, where it is proportional to the square of time. It will be a benefit for future high-speed quantum search. Electric circuits have a merit that they are easily equipped compared with other methods such as photonic, wave-guide and nuclear-magnetic resonant systems. Furthermore, there is a potentiality to construct integrated circuits of quantum walks.

The author is very much grateful to N. Nagaosa and E. Saito for helpful discussions on the subject. This work is supported by the Grants-in-Aid for Scientific Research from MEXT KAKENHI (Grants No. JP17K05490, No. JP15H05854 and No. JP18H03676). This work is also supported by CREST, JST (JPMJCR16F1).

-
- ¹ C. H. Lee, S. Imhof, C. Berger, F. Bayer, J. Brehm, L. W. Molenkamp, T. Kiessling and R. Thomale, *Communications Physics*, **1**, 39 (2018).
 - ² S. Imhof, C. Berger, F. Bayer, J. Brehm, L. Molenkamp, T. Kiessling, F. Schindler, C. H. Lee, M. Greiter, T. Neupert, R. Thomale, *Nat. Phys.* **14**, 925 (2018).
 - ³ M. S.-Garcia, R. Susstrunk and S. D. Huber, *Phys. Rev. B* **99**, 020304 (2019).
 - ⁴ T. Helbig, T. Hofmann, C. H. Lee, R. Thomale, S. Imhof, L. W. Molenkamp and T. Kiessling, *Phys. Rev. B* **99**, 161114 (2019).
 - ⁵ Y. Lu, N. Jia, L. Su, C. Owens, G. Juzeliunas, D. I. Schuster and J. Simon, *Phys. Rev. B* **99**, 020302 (2019).
 - ⁶ M. Ezawa, *Phys. Rev. B* **98**, 201402(R) (2018).
 - ⁷ T. Hofmann, T. Helbig, C. H. Lee, M. Greiter, R. Thomale, *Phys. Rev. Lett.* **122**, 247702 (2019).
 - ⁸ K. Luo, R. Yu and H. Weng, *Research* (2018), ID 6793752.
 - ⁹ M. Ezawa, *Phys. Rev. B* **99**, 201411(R) (2019).
 - ¹⁰ M. Ezawa, *Phys. Rev. B* **99**, 121411(R) (2019).
 - ¹¹ M. Ezawa, *Phys. Rev. B* **100**, 081401(R) (2019).
 - ¹² M. Ezawa, *Phys. Rev. B* **100**, 045407 (2019).
 - ¹³ T. Helbig, T. Hofmann, S. Imhof, M. Abdelghany, T. Kiessling, L. W. Molenkamp, C. H. Lee, A. Szameit, M. Greiter, R. Thomale, *arXiv:1907.11562*
 - ¹⁴ Q.-B. Zeng, Y.-B. Yang and Y. Xu, *arXiv:1901.08060*
 - ¹⁵ H. Jiang, L.-J. Lang, C. Yang, S.-L. Zhu and S. Chen, *arXiv:1901.09399*
 - ¹⁶ C. H. Lee, T. Hofmann, T. Helbig, Y. Liu, X. Zhang, M. Greiter and R. Thomale, *cond-mat/arXiv:1904.10183*
 - ¹⁷ Y. Aharonov, L. Davidovich and N. Zagury, *Phys. Rev. A*, **48**, 1687 (1993).
 - ¹⁸ E. Farhi and S. Gutmann, *Phys. Rev. A* **58**, 915 (1998)
 - ¹⁹ A. Ambainis, *Int. J. Quantum Information*, **1**, 507 (2003)
 - ²⁰ S. E. Venegas-Andraca, *Quantum Information Processing*, **11**, 1015 (2012)
 - ²¹ J. Kempe, *Contemporary Physics* **44**, 307 (2003)
 - ²² M. S. Rudner and L. S. Levitov, *Phys. Rev. Lett.* **102**, 065703 (2009).
 - ²³ D. ben-Avraham, E. M. Boltt and C. Tamon, *Quantum Information Processing*, **3**, 1 (2004)
 - ²⁴ N. Konno, *Phys. Rev. E*, **72** 026113 (2005)
 - ²⁵ M. Szegedy, in *Proceedings of the 45th IEEE Symposium on Foundations of Computer Science (IEEE, New York, 2004)*, pp. 32-41.
 - ²⁶ A. M. Childs, *Phys. Rev. Lett.* **102**, 180501 (2009).
 - ²⁷ A. M. Childs, D. Gosset, Z. Webb, *Science* **339**, 791 (2013)
 - ²⁸ Z. H. Bian, J. Li, H. Qin, X. Zhan, R. Zhang, B. C. Sanders, and P. Xue, *Phys. Rev. Lett.* **114**, 203602 (2015)
 - ²⁹ A. Peruzzo, M. Lobino, J. C. F. Matthews, N. Matsuda, A. Politi, K. Poulios, X.-Q. Zhou, Y. Lahini, N. Ismail, K. Worhoff, Y. Bromberg, Y. Silberberg, M. G. Thompson, J. L. O'Brien, *Science*, **329**(5998):1500, (2010)
 - ³⁰ A. A. Guzik and P. Walther, *Nature Physics* **8**, 285 (2012)

- ³¹ T. Kitagawa, M. A. Broome, A. Fedrizzi, M. S. Rudner, E. Berg, I. Kassal, A. Aspuru-Guzik, E. Demler and A. G. White, *Nature Communications* **3**, 882 (2012)
- ³² L. Xiao, X. Zhan, Z. H. Bian, K. K. Wang, X. Zhang, X. P. Wang, J. Li, K. Mochizuki, D. Kim, N. Kawakami, W. Yi, H. Obuse, B. C. Sanders, and P. Xue, *Nat. Physics* **13**, 1117 (2017).
- ³³ H. B. Perets, Y. Lahini, F. Pozzi, M. Sorel, R. Morandotti and Y. Silberberg, *Phys. Rev. Lett.* **100**, 170506 (2008)
- ³⁴ J. Du, H. Li, X. Xu, M. Shi, J. Wu, X. Zhou and R. Han, *Phys. Rev. A* **67**, 042316 (2003)
- ³⁵ M. S. Rudner and L. S. Levitov, *Phys. Rev. B* **82**, 155418 (2010)
- ³⁶ E. I. Rosenthal, N. K. Ehrlich, M. S. Rudner, A. P. Higginbotham, and K. W. Lehnert, *Phys. Rev. B* **97**, 220301(R) (2018)
- ³⁷ N. Hatano and D. R. Nelson, *Phys. Rev. Lett.* **77**, 570 (1996); *Phys. Rev. B* **56**, 8651 (1997); *Phys. Rev. B* **58**, 8384 (1998).
- ³⁸ Z. Gong, Y. Ashida, K. Kawabata, K. Takasan, S. Higashikawa and M. Ueda, *Phys. Rev. X* **8**, 031079 (2018).
- ³⁹ C. H. Lee, L. Li and J. Gong, *Phys. Rev. Lett.* **123**, 016805 (2019).